The Astrophysical Journal, 889:156 (11pp), 2020 February 1 https://doi.org/10.3847/1538-4357/ab6730

The Roles of Mass and Environment in the Quenching of Galaxies. II.

E. Contini[1], Q. Gu[1], X. Ge[1], J. Rhee[2], S. K. Yi[2], and X. Kang[3]
[1] School of Astronomy and Space Science, Nanjing University, Nanjing 210093, People's Republic of China; emanuele.contini82@gmail.com; qsgu@nju.edu.cn
[2] Department of Astronomy and Yonsei University Observatory, Yonsei University, Yonsei-ro 50, Seoul 03722, Republic Of Korea
[3] Purple Mountain Observatory, the Partner Group of MPI für Astronomie, 2 West Beijing Road, Nanjing 210008, People's Republic of China
Received 2019 October 28; revised 2019 December 12; accepted 2019 December 28; published 2020 February 4

Abstract

We take advantage of an analytic model of galaxy formation coupled to the merger tree of an *N*-body simulation to study the roles of environment and stellar mass in the quenching of galaxies. The model has been originally set in order to provide the observed evolution of the stellar mass function as well as reasonable predictions of the star formation rate–stellar mass relation, from high redshift to the present time. We analyze the stellar mass and environmental quenching efficiencies and their dependence on stellar mass, halo mass (taken as a proxy for the environment), and redshift. Our analysis shows that the two quenching efficiencies are dependent on redshift and stellar and halo mass, and that the halo mass is also a good proxy for the environment. The environmental quenching increases with decreasing redshift and is inefficient below $\log M_* \sim 9.5$, reaches the maximum value at $\log M_* \sim 10.5$, and decreases again, becoming poorly efficient at very high stellar mass ($\log M_* \gtrsim 11.5$). Central and satellites galaxies are mass quenched differently: for the former, the quenching efficiency depends very weakly on redshift but strongly on stellar mass; for the latter, it strongly depends on both stellar mass and redshift in the range $10 \lesssim \log M_* \lesssim 11$. According to the most recent observational results, we find that the two quenching efficiencies are not separable: intermediate-mass galaxies, as well as intermediate/massive galaxies in more massive halos, are environmentally quenched faster. At stellar masses lower than $\log M_* \lesssim 9.5$, both quenching mechanisms become inefficient, independently of the redshift.

Unified Astronomy Thesaurus concepts: Galaxy formation (595); Galaxy evolution (594)

1. Introduction

During the last decades, the scientific community has spent a considerable amount of effort and resources to learn more about the physical processes that drive galaxy formation and evolution and, among them, those responsible for the quenching of the star formation activity in galaxies, which is fundamentally important. Galaxy quenching is, indeed, thought to have a remarkable role in shaping galaxy properties, such as morphology, colors, and stellar age (Blanton et al. 2003; Baldry et al. 2004; Balogh et al. 2004; Brinchmann et al. 2004; Kauffmann et al. 2004; Cassata et al. 2008; Muzzin et al. 2012, 2013; Davies et al. 2019; Pallero et al. 2019, and others).

Nowadays, we all agree that galaxies can be roughly classified into two main categories according to their main properties: on one hand, we have star-forming systems, which are galaxies that are forming stars, have blue colors, are typically young, and that show late-type morphologies; on the other hand, we find quiescent or passive systems, which are galaxies with no or little star formation activity, have red colors and typically old stellar ages, and show early-type morphologies (Blanton et al. 2003; Kauffmann et al. 2003; Baldry et al. 2004; Noeske et al. 2007; Gallazzi et al. 2008; Wuyts et al. 2011; Wetzel et al. 2012; van der Wel et al. 2014). Similarly, the same properties are found to be also dependent on stellar mass and environment in such a way that galaxies living in a denser environment or that are more massive are typically early-type systems, less star-forming, redder, with old stellar ages, and are more metal-rich (Dressler 1980; Kauffmann et al. 2003, 2004; Baldry et al. 2006; Weinmann et al. 2006; Bamford et al. 2009; Cooper et al. 2010; Peng et al. 2010; von der Linden et al. 2010).

It appears clear that physical processes that are related to both the surroundings of a given galaxy and its internal conditions play a role in quenching its star formation. We usually adopt the term "environmental quenching" when we refer to the former and "mass quenching" for the latter (Peng et al. 2010). These two modes of quenching together are responsible for the star formation history of galaxies, and, although there is not yet a general consensus, there is evidence that they play different roles at different times and stellar masses (Muzzin et al. 2012; Peng et al. 2012; Balogh et al. 2016; Darvish et al. 2016; Kawinwanichakij et al. 2017; Papovich et al. 2018; Contini et al. 2019a; Pintos-Castro et al. 2019, and references therein).

The term "mass quenching" collects all the internal processes that mainly depend on, or are linked to, the galaxy mass, such as gas outflows driven by stellar winds or supernova explosions (Larson 1974; Dekel & Silk 1986; Dalla Vecchia & Schaye 2008), or active galactic nucleus (AGN) feedback from the central supermassive black hole (Croton et al. 2006; Fabian 2012; Fang et al. 2013; Cicone et al. 2014; Bremer et al. 2018). On the other hand, the term "environmental quenching" pertains to the physical processes that quench galaxies because of their interaction with the surrounding area, such as ram pressure stripping (Gunn & Gott 1972), starvation (or strangulation; Larson et al. 1980), and harassments (Moore et al. 1996).

What process/es, i.e., environmental or mass driven, dominate the quenching of galaxies is still unclear and under debate. It is generally thought that mass quenching dominates in massive galaxies and especially at high redshift, while environmental quenching becomes important at redshift $z \lesssim 1$ (e.g., Peng et al. 2010). Moreover, it has become clear that, in order to see their single effects, both quenching mechanisms have to be studied separately, that is, trying to separate the contribution of one while studying the effect of the other (see,

e.g., Muzzin et al. 2012; Darvish et al. 2016; Pintos-Castro et al. 2019). Both mechanisms can be studied by looking at how the star formation rate (SFR) or specific SFR (SSFR) depend on environment, which can be defined as the halo mass, clustercentric distance, or the surrounding density, and on stellar mass. Another direct way would be by computing their efficiencies, as defined, for example, in van den Bosch et al. (2008) or Peng et al. (2010; but see also Balogh et al. 2016; Darvish et al. 2016; Fossati et al. 2017; Pintos-Castro et al. 2019 and others), and in particular on how they depend on stellar mass, halo mass (or any other proxy for the environment), and redshift.

The two ways together are, in principle, supposed to give more information regarding the relative roles of the two quenching modes. For instance, concerning the environmental quenching, when we look at the dependence of the SFR or SSFR on the environment since redshift $z \sim 1$ (when the environment is believed to play a remarkable role), we find no dependence (see, e.g., Muzzin et al. 2012; Laganá & Ulmer 2018; Contini et al. 2019a, and references therein for many other works supporting it), which either means that the environment does not play an important role or it acts so fast such that it does not influence the star formation of active galaxies but increases the fraction of quiescent galaxies. Many other studies (e.g., van den Bosch et al. 2008; Quadri et al. 2012; Omand et al. 2014; Balogh et al. 2016; Darvish et al. 2016; Nantais et al. 2016; Fossati et al. 2017; Jian et al. 2017; Kawinwanichakij et al. 2017; Papovich et al. 2018; van der Burg et al. 2018; Pintos-Castro et al. 2019), which have looked at the efficiencies of environmental and mass quenching, have been able to quantify the two quenching modes, albeit with different results in terms of mutual dependence among the two modes, and redshift, stellar mass, and halo mass dependence. This reasoning highlights the importance of a quantity that is able to capture the level of quenching, given both by the environment and stellar mass.

What can add more information about quenching mechanisms is given by the mutual dependence of the two efficiencies and by how each of them depends on redshift. There are observational results supporting the idea that the two quenching processes are separable, such as in Baldry et al. (2006), van den Bosch et al. (2008), Peng et al. (2010), Quadri et al. (2012), Kovač et al. (2014), and van der Burg et al. (2018), and more recent works claiming that they are not, such as Balogh et al. (2016), Darvish et al. (2016), Fossati et al. (2017), Kawinwanichakij et al. (2017), Papovich et al. (2018), Pintos-Castro et al. (2019), and Chartab et al. (2019). Similarly, concerning the redshift dependence: the environmental (or mass) quenching efficiency is found to be dependent on redshift in several studies (such as Darvish et al. 2016; Nantais et al. 2016; Fossati et al. 2017; Jian et al. 2017; Pintos-Castro et al. 2019), and not dependent in others (such as Quadri et al. 2012; Balogh et al. 2016).

In Contini et al. (2019a; hereafter PapI) we took advantage of an analytic model of galaxy formation that was tuned to match the observed evolution of the stellar mass function from redshift $z \sim 2.3$ down to the present time and give a reasonable prediction of the evolution of the SFR–M_* relation in the same redshift range, to investigate galaxy quenching by looking at the SFR and SSFR of star-forming and quiescent galaxies as a function of both stellar mass and environment. Our goal was mainly to understand the roles of environmental and mass quenching at different redshifts. We concluded that stellar mass is the main parameter responsible for the quenching of galaxies at any redshift investigated (from $0 < z < 1.5$), and the environment is just secondary. However, we pointed out the necessity of a further analysis by looking at the efficiencies of the two quenching modes which, as explained above, can give much more information and better quantify the roles of mass and environment. The aim of the current paper is to address this point, by analyzing the two quenching efficiencies and their dependences on stellar mass, halo mass, and redshift, in order to shed more light and put some constraints on the possible physical mechanisms that quench galaxies, and on their relative importance as a function of time.

This paper is organized as follows. In Section 2, we briefly describe our model and define the quenching efficiencies. In Section 3, we present our analysis, which will be fully discussed in Section 4, and in Section 5, we draw our conclusions. Throughout this paper, we use a standard cosmology, namely $\Omega_\lambda = 0.73$, $\Omega_m = 0.27$, $\Omega_b = 0.044$, $h = 0.7$, and $\sigma_8 = 0.81$. Stellar masses are computed with the assumption of a Chabrier (2003) initial mass function, and all units are h corrected.

2. Methods

In the analysis done in PapI, we made use of an analytic model that was previously developed in Contini et al. (2017a) and later refined in Contini et al. (2017b). The model ran on the merger tree of an N-body simulation presented in Kang et al. (2012), with the main goals of predicting the observed evolution of the stellar mass function and giving a reasonable prediction of the SFR–M_* relation as a function of redshift. For what concerns the topic addressed here, a sufficient description of the model can be found in PapI, while we refer the reader to Contini et al. (2017b) for a detailed explanation. Here we briefly put into words the main characteristics and implementations important in the context of this paper.

The main feature of the model is to make use of the subhalo abundance matching technique to populate dark matter halos with galaxies (e.g., Vale & Ostriker 2004). The model reads the merger tree of the N-body simulation where all the information regarding the merger history of each halo is stored. At one particular redshift, which we set to $z_{\rm match} = 2.3$, the model is forced to match the observed stellar mass function. At redshifts lower than $z_{\rm match}$, the code sorts newborn dark matter halos and, by using the stellar mass–halo mass relation at that particular redshift, it assigns a galaxy to each halo. The two novelties of the implementation rely on the way we treat (1) the merger histories of a galaxy and (2) its star formation history.[4] The former is given directly by the information stored in the merger tree, while the latter is treated with a functional form (see Equations (1)–(3) in PapI), which is different according to the type of the galaxy (central or satellite) and depends on the quenching timescale (function of stellar mass, redshift, and type of galaxy). For what concerns the treatment of the star formation history, the philosophy of our model is very similar to the so-called "delayed-then-rapid" quenching mode suggested by Wetzel et al. (2013), where satellites evolve as

[4] It must be noted that the model also considers the formation of the intracluster light via stellar stripping and galaxy mergers (see Contini et al. 2014, 2018, 2019b for more details).

centrals for a given amount of time (delay) after accretion, and then quench fast right after (rapid mode).

2.1. Quenching Efficiencies

In order to quantify the quenching due to the environment and stellar mass, in the following analysis we make use of two quantities: the environmental quenching efficiency, $\epsilon_{\rm env}$, and the mass quenching efficiency, $\epsilon_{\rm mass}$. The two quantities were originally introduced by Peng et al. (2010; although a similar approach for the environmental quenching efficiency was introduced earlier by van den Bosch et al. 2008), and later used by other authors (e.g., Quadri et al. 2012; Kovač et al. 2014; Balogh et al. 2016; Kawinwanichakij et al. 2017; Pintos-Castro et al. 2019) to quantify the relative role of mass and environment in quenching galaxies, even though with slightly different definitions.

We define the environmental quenching efficiency as follows:

$$\epsilon_{\rm env}(M_h, M_{h,0}, M_*, z) = \frac{f_q(M_h, M_*, z) - f_q(M_{h,0}, M_*, z)}{1 - f_q(M_{h,0}, M_*, z)}, \quad (1)$$

where $f_q(M_h, M_*, z)$ is the fraction of quiescent galaxies of mass M_* in halos of mass M_h at redshift z, $f_q(M_{h,0}, M_*, z)$, the same fraction but for quiescent galaxies in low-mass halos ($M_h < 10^{13} M_\odot$). Basically, for galaxies in a given environment defined as the halo mass, $\epsilon_{\rm env}$ quantifies the excess (with respect to what we will refer to as field environment) of galaxies that are quenched because of physical processes linked to the environment at redshift z. In practice, we divide the sample of galaxies into centrals and satellites. Centrals are selected as field galaxies, i.e., residing in very low-mass halos ($M_h < 10^{13} M_\odot$) with no or a few satellites around, while satellites are taken within the virial radius R_{200} of halos with $M_h > 10^{13} M_\odot$. It is worth noting that, among centrals, the brightest group/cluster galaxies (i.e., those residing in the center of the main halos) are not included in the analysis. For this reason, centrals are real "field/isolated" galaxies. For the sake of simplicity, in the rest of paper we will call them "centrals" or "field galaxies."

Similarly, the mass quenching efficiency is defined as

$$\epsilon_{\rm mass}(M_*, M_{*,0}, M_h, z) = \frac{f_q(M_h, M_*, z) - f_q(M_h, M_{*,0}, z)}{1 - f_q(M_h, M_{*,0}, z)}, \quad (2)$$

where $f_q(M_h, M_*, z)$ is the fraction of quiescent galaxies of mass M_* in halos of mass M_h at redshift z, and $f_q(M_h, M_{*,0}, z)$ is the fraction of quiescent galaxies in the same fixed environment given by M_h at a lower stellar mass $M_{*,0}$. Essentially, at a fixed environment, $\epsilon_{\rm mass}$ quantifies the fraction of galaxies that have been quenched compared to the star-forming fraction at lower stellar mass ($M_{*,0}$). In the literature, the completeness limit at a given redshift is often chosen as the reference stellar mass $M_{*,0}$ (see, e.g., Darvish et al. 2016; Kawinwanichakij et al. 2017; Pintos-Castro et al. 2019). Given the fact that our completeness limit (at any redshift) is far lower than that of the above-quoted works, we choose $M_{*,0}$ as the stellar mass at which at least 90% of the galaxies are star-forming. However, as we will see below, our model overestimates the SFR for low-mass galaxies, so our choice translates into $\log M_{*,0} \simeq 9.6$–9.7 for satellites in the redshift range considered (except for $z = 1.5$ for which $\log M_{*,0} \sim 10.4$), and $\log M_{*,0} \simeq 10.5$ for centrals, similar to $M_{*,0}$ of many observational studies.

There are some caveats concerning the definitions of the two efficiencies that are worth mentioning. The first one is with regard to the definition of the environmental quenching efficiency $\epsilon_{\rm env}$. The excess of galaxies that are quenched with respect to the field, and in our case the excess of satellites (cluster environment) with respect to centrals (field), is calculated at the same epoch. As many authors noted (e.g., Balogh et al. 2016; van der Burg et al. 2018), a better approach would be to consider the quenched fraction in the field at the time of accretion. Theoretically speaking, this would be possible with models of galaxy formation that are able to trace the history of any single galaxy, such as ours, but observationally impossible without assumptions (which anyway would not avoid the progenitor bias issue) on the different galaxy populations. In the following analysis, we decide to keep the same observational approach (the classical definition) to have fair comparisons with observational works. Another important issue concerning the definition of $\epsilon_{\rm env}$ relies on the fact that it does not consider the differential growth in stellar mass of galaxies, which might not be negligible, simply because the two populations are taken at the same redshift.

There is a second issue regarding the definitions of both efficiencies, which makes direct comparisons not simple and relies on the definition of the environment itself. As noted in PapI, the definition of the environment in the literature spans from the mass of the halo where the galaxy resides to the clustercentric distance or local galaxy density. In this work, we first separate satellite from central galaxies, which already is a first level of environmental separation, and then, among satellites, we define their environment by using their halo mass (not to be confused with their subhalo mass) as a proxy.

Having in mind the discussion above, in the following section we present our analysis where we focus mainly on

(a) quantifying the environmental quenching efficiency $\epsilon_{\rm env}$ and its dependence on redshift and halo mass;
(b) quantifying the mass quenching efficiency $\epsilon_{\rm mass}$ and its dependence on redshift and stellar mass;
(c) the mutual dependence of the two efficiencies, i.e., whether or not $\epsilon_{\rm env}$ depends on stellar mass and $\epsilon_{\rm mass}$ depends on the environment.

Given the different results found in the recent past, point (c) is particularly interesting. The case of mutual dependence of the two efficiencies would mean that the two quenching modes are not separable.

3. Results

In this section, we present the main results of our model, and their interpretation will be discussed in Section 4, which will also consider a full comparison with the most relevant works. As we need to separate star-forming from quiescent galaxies, we decide to follow the same approach used in PapI, i.e., we use an SSFR cut that is redshift dependent. At a given redshift, we consider star-forming all those galaxies with SSFR higher

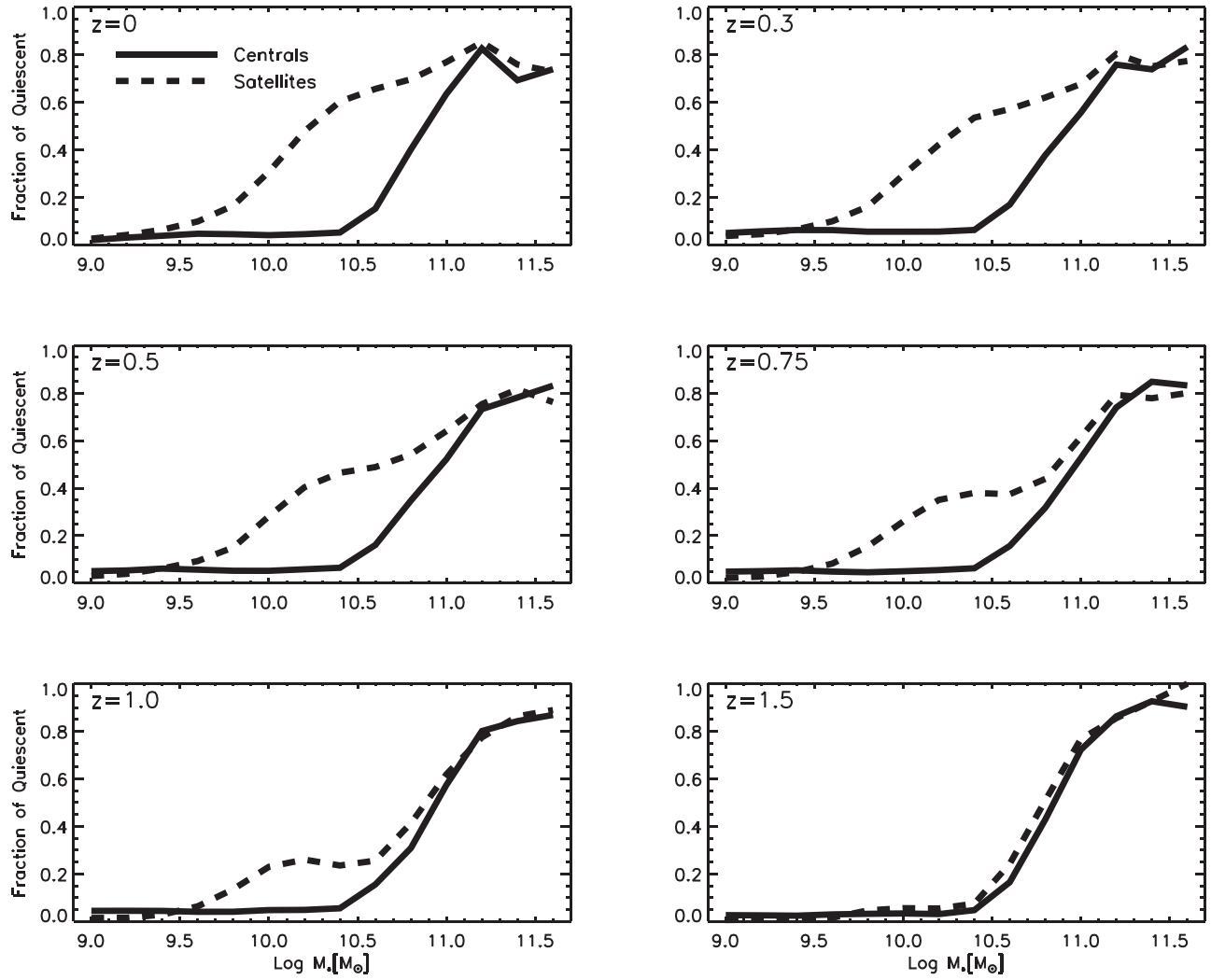

Figure 1. Fraction of quiescent central (solid lines) and satellite (dashed lines) galaxies as a function of stellar mass at different redshifts (different panels), from $z = 1.5$ to $z = 0$. The fraction of quenched satellites is higher than the fraction of quenched centrals at almost all masses ($\log M_* \simeq$ [9.5–11]) and redshifts ($z =$ [0.0–1.0]).

than $t_{\rm hubble}^{-1}$ and quiescent all those with SSFR lower than that. In order to study the effect of the environment, we split our sample of galaxies according to their rank, central or satellites. As mentioned above, centrals are isolated galaxies, which we consider as the "field" environment, while satellites are galaxies that reside within the virial radius of groups/clusters with mass higher than $10^{13}\,M_\odot$. For satellites, we will consider the effect of being part of groups/clusters of different mass because the halo mass is our proxy for the environment.

Figure 1 plots the fraction of quiescent central (solid lines) and satellite (dashed lines) galaxies as a function of stellar mass at different redshifts (different panels), from $z = 1.5$ to $z = 0$. We note that there is a clear dependence on stellar mass for both types of galaxies, being a fraction higher at increasing stellar mass, independent of the redshift. Moreover, in the redshift range $z =$ [0.0–1.0] (i.e., with the only exception of $z = 1.5$), the fraction of quenched satellites is higher than that of quenched centrals at almost all stellar masses ($\log M_* \simeq$ [9.5–11]), except for low- and high-mass galaxies. Compared with most of the observational fractions, the predictions of our model are low in the low-mass end. As we pointed out in PapI, the different definitions for separating star-forming from quiescent galaxies can play a significant role, but we also noticed that our model could overestimate the SFR history of low-mass galaxies. This problem, if real, can bias the efficiency of quenching (both environmental and mass) for galaxies with low stellar mass. Having in mind this caveat, in the following two subsections we present a detailed analysis of the quenching modes by studying the dependences of $\epsilon_{\rm env}$ and $\epsilon_{\rm mass}$ on stellar mass, halo mass, and redshift.

3.1. Environmental Quenching Efficiency

We make use of Equation (1) to derive the environmental quenching efficiency $\epsilon_{\rm env}$ and plot it as a function of stellar mass at different redshifts in the left panel of Figure 2. $\epsilon_{\rm env}$ clearly depends on redshift, being higher with decreasing redshift, and on stellar mass, being lower for low- and high-mass galaxies. The trend with redshift that we find is in agreement with many other works (see, e.g., Darvish et al. 2016; Nantais et al. 2016; Fossati et al. 2017), but in disagreement with others (e.g., Quadri et al. 2012; Balogh et al. 2016). However, it must be noted that there is a growing consensus for increasing efficiency with decreasing redshift, as one would expect if the environment plays a more important role at low redshift.

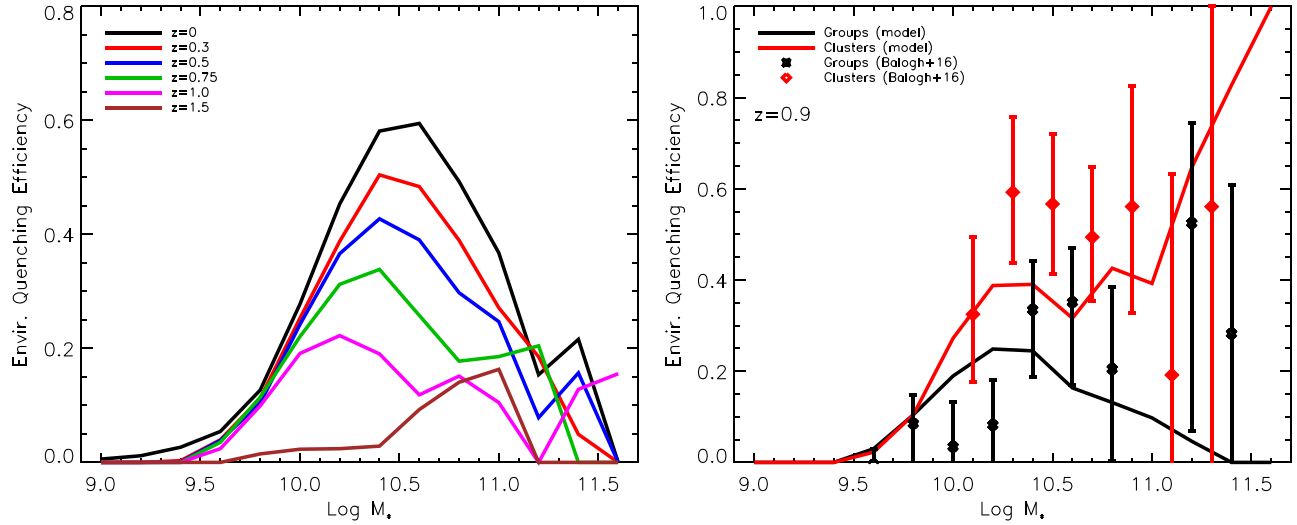

Figure 2. Left panel: environmental quenching efficiency as a function of stellar mass at different redshifts (different colors), from $z = 1.5$ to $z = 0$. Right panel: environmental quenching efficiency as a function of stellar mass at $z = 0.9$, for groups (black line) and clusters (red line) as predicted by our model and compared with observed data (black crosses and red diamonds) by Balogh et al. (2016) in the same redshift ($0.8 < z < 1.2$) and halo mass ranges ($13.5 < \log M_{\rm halo} < 14.0$ for groups, and $\log M_{\rm halo} > 14.2$ for clusters).

The dependence of $\epsilon_{\rm env}$ on stellar mass is a more delicate issue. In the right panel of Figure 2, we compare the dependence of $\epsilon_{\rm env}$ on stellar mass as predicted by our model with observational results by Balogh et al. (2016), for groups (black line and crosses) and clusters (red line and diamonds) at redshift $z \sim 0.9$. Groups and clusters have been chosen in the same redshift range ($0.8 < z < 1.2$) and halo mass ranges as in Balogh et al., i.e., $13.5 < \log M_{\rm halo} < 14.0$ for groups, and $\log M_{\rm halo} > 14.2$ for clusters. The predictions of our model agree fairly well with the observed data, in particular the decrease of the efficiency at lower stellar mass in groups. Balogh et al. (2016) find that the environmental quenching efficiency decreases with stellar mass and becomes inefficient at $\log M_* < 9.5$. Their results are supported by Papovich et al. (2018), who study the effect of the environment in shaping the evolution of the stellar mass function in the redshift range $0.2 < z < 2.0$, and find that the evolution of the stellar mass function of quiescent galaxies implies a decreasing $\epsilon_{\rm env}$ with decreasing stellar mass. Our model is in line with this picture and, considering the caveat discussed above (the overestimation of the SFR of low-mass galaxies discussed in Section 3), it is evidence that our results are safe even at low stellar mass. Moreover, although from the left panel of Figure 2 we see that the $\epsilon_{\rm env}$ of high-mass galaxies is low compared to intermediate-mass galaxies, in the right panel, we show that the environmental efficiency of high-mass galaxies in clusters is higher than that of high-mass galaxies in groups. We will come back to this, and discuss both points below, where we will provide more evidence supporting these results.

Now we study the dependence of the environmental quenching efficiency on the halo mass, as a function of redshift and at fixed stellar mass. This information is shown in the two panels of Figure 3, for galaxies with stellar mass in the range $9.5 < \log M_* < 10.5$ (left panel), and $10.5 < \log M_* < 11.5$ (right panel). As in the previous figure, the efficiency is higher at lower redshift, but there are two points worth noting from the information given by this figure: (a) the efficiency does not depend on halo mass (i.e., environment) for the lowest stellar mass galaxies and (b) it does in the highest stellar mass galaxies, regardless of the redshift. For instance, while in the left panel the efficiency at the present time is basically constant at the value ∼0.25, in the right panel it spans the range 0.2 in low-mass halos to 0.6 in high-mass halos. This is clear evidence that the environment acts differently on galaxies of different mass. To summarize so far, the environmental quenching efficiency is stellar mass dependent and also environmental dependent.

We conclude the analysis concerning the environmental quenching efficiency with Figure 4, which plots the integrated $\epsilon_{\rm env}$ as a function of redshift for clusters (left panel) and groups (right panel). Our model (solid black lines) is compared with several observations (different points and shaded regions). For the sake of honesty, we must stress that these comparisons are not 100% fair for three simple reasons: different authors have different stellar mass completeness limits in deriving $\epsilon_{\rm env}$ and the halo mass ranges (group or cluster) are also different (we used the same ranges of halo mass adopted in Figure 2). Moreover, the proxy for the environment is also different from author to author (e.g., halo mass, local density, and cluster-centric distance) and yields to different definitions of $\epsilon_{\rm env}$. Given these caveats, we can reasonably state that our model predicts the observed trend with redshift and matches most of the observations from high redshift to the present time, in groups and clusters.

In order to highlight the most important results so far, we can simply summarize as follows: the environmental quenching efficiency is dependent on redshift, stellar mass, and environment.

3.2. Mass Quenching Efficiency

Analogously to the analysis done in the previous subsection, here we make use of Equation (2) to derive the mass quenching efficiency, and study its dependence on redshift, stellar, and halo mass. In Figure 5, we show $\epsilon_{\rm mass}$ as a function of stellar mass for central (left panel) and satellite (right panel) galaxies, at different redshifts as indicated in the legend.[5] The plots show

[5] The stellar mass ranges in the two panels are different because central galaxies below $\log M_* \sim 10.4$ and satellite galaxies below $\log M_* \sim 9.5$ are all star-forming.

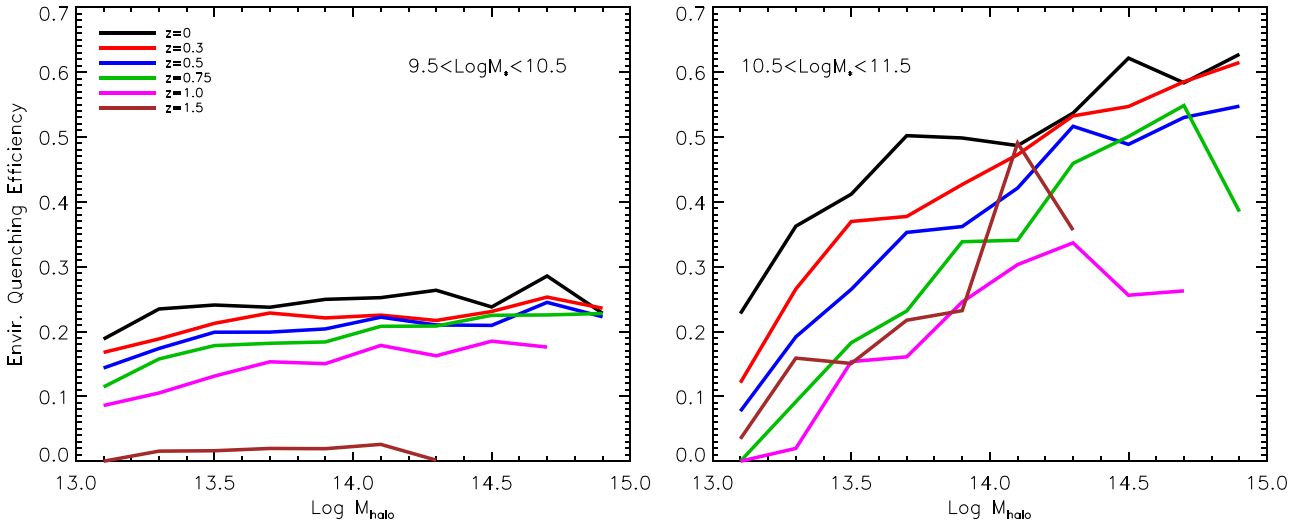

Figure 3. Environmental quenching efficiency as a function of halo mass at different redshifts (different colors), for galaxies in two stellar mass ranges (different panels). The efficiency of environmental quenching does not depend strongly on the halo mass for low-mass galaxies, while it strongly depends on halo mass for more massive galaxies. In both stellar mass ranges, a redshift dependence is seen, that is, the efficiency is higher with decreasing redshift.

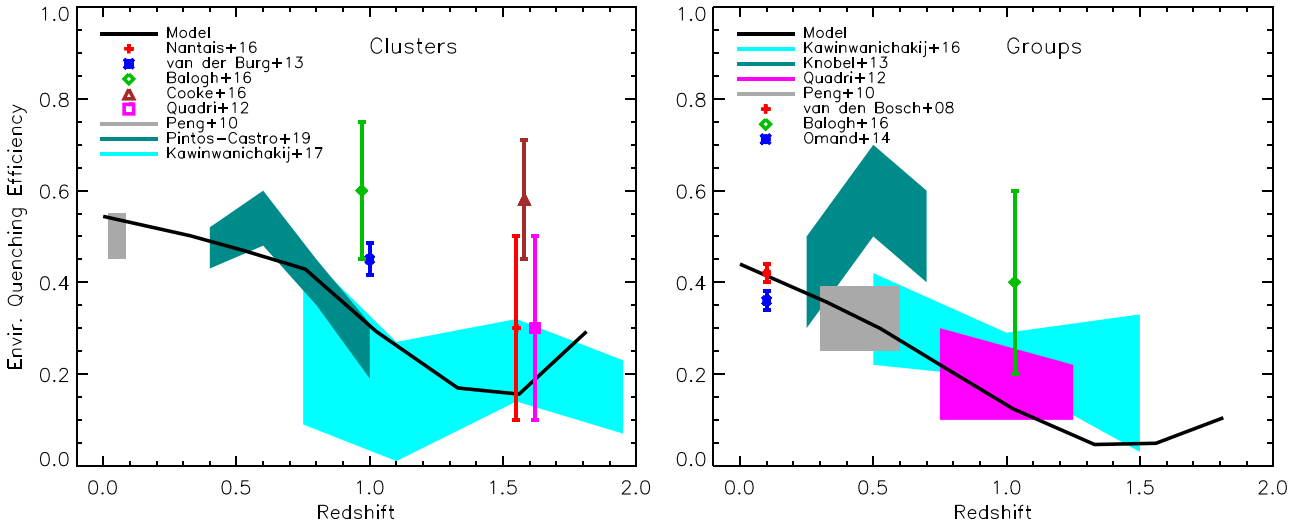

Figure 4. Environmental quenching efficiency as predicted by the model (solid lines) as a function of redshift in clusters (left panel) and groups (right panel), compared with several observed data. Overall, our model is able to reproduce the observed trend (lower efficiency with increasing redshift) in both groups and clusters.

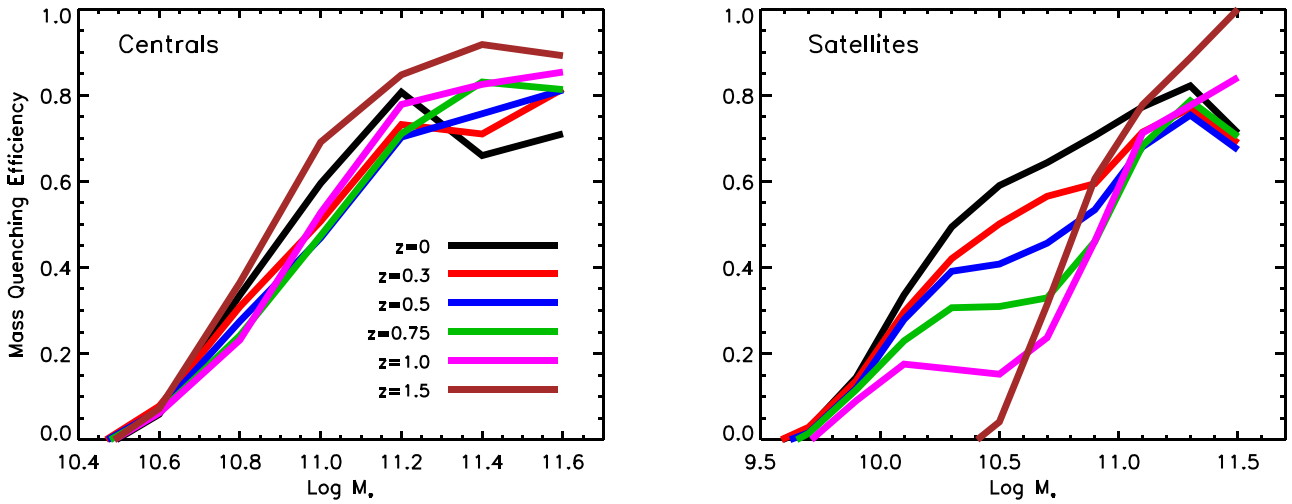

Figure 5. Mass quenching efficiency as a function of stellar mass at different redshifts (different colors), for central (left panel) and satellite (right panel) galaxies. There is a clear trend with stellar mass, in that more massive galaxies are more efficiently quenched by internal processes, for both centrals and satellites. Moreover, although the dependence on redshift is not clear for centrals, satellites in the intermediate–massive stellar mass range are more efficiently quenched at lower redshift.

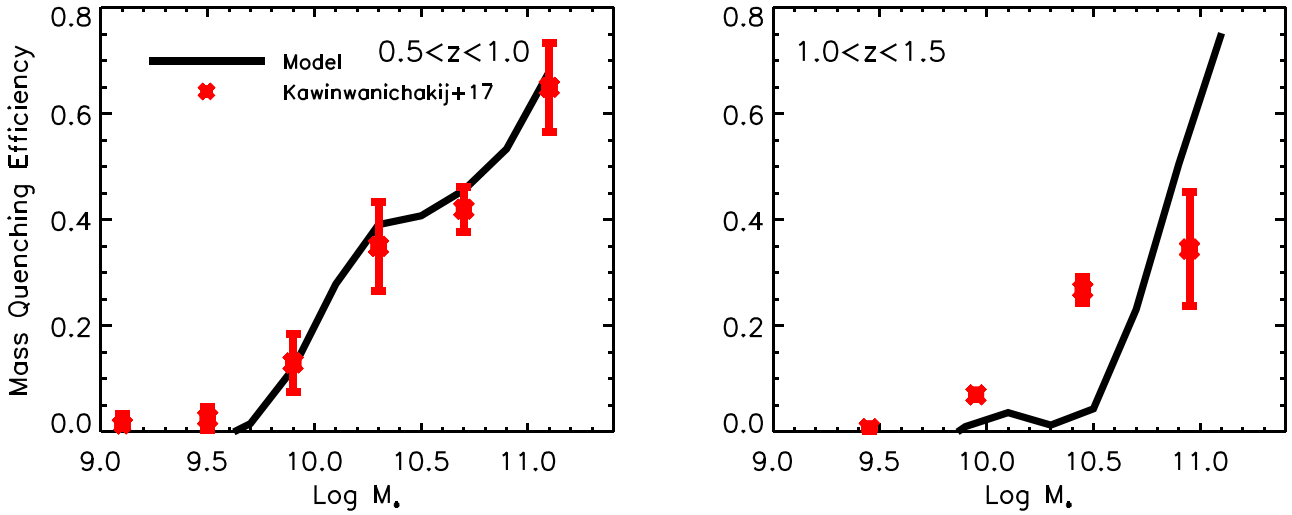

Figure 6. Comparison of the predictions of our model with the observed data by Kawinwanichakij et al. (2017) for the mass quenching efficiency as a function of stellar mass in two redshift ranges (different panels), $0.5 < z < 1.0$ and $1.0 < z < 1.5$. Our model matches very well the observed data in the lowest redshift range, and although it captures the overall trend with stellar mass even at higher redshift (increasing efficiency with increasing stellar mass), it does not match the observed data. In order to be as consistent as possible with the observed data (galaxies in the highest density environments of Kawinwanichakij et al.'s (2017) sample), the predictions of the model consider only satellite galaxies.

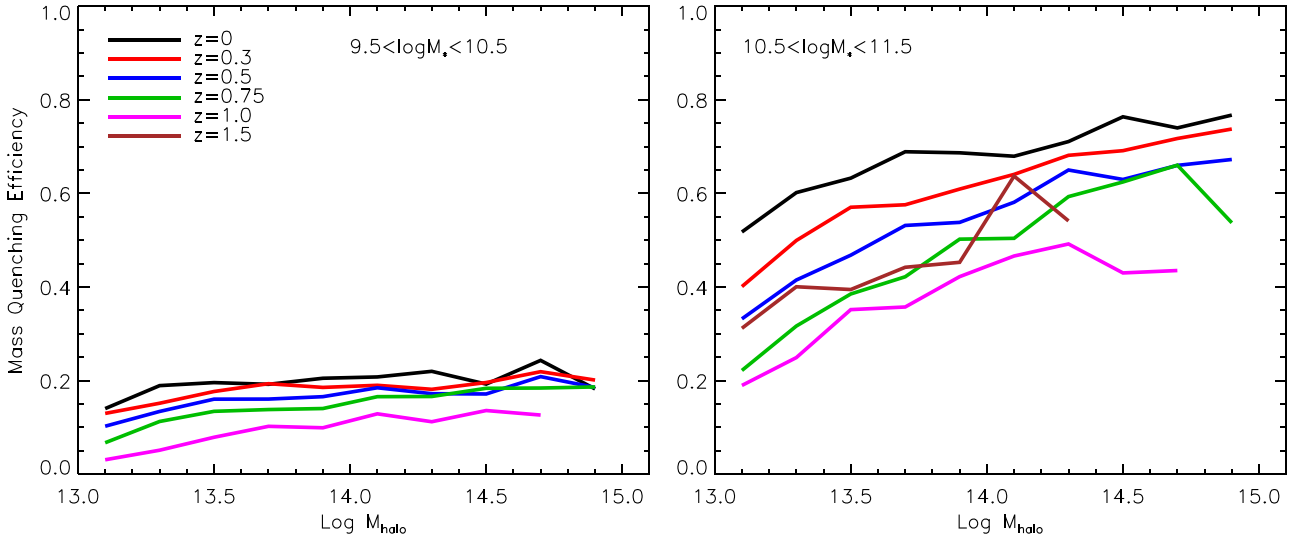

Figure 7. Mass quenching efficiency as a function of halo mass at different redshifts (different colors), for galaxies in two stellar mass ranges (different panels). The efficiency of mass quenching does not depend strongly on the halo mass for low-mass galaxies, while it does depend on halo mass for more massive galaxies. Similarly to Figure 3 (environmental quenching efficiency as a function of halo mass), the efficiency is redshift dependent, being higher with decreasing redshift.

a clear dependence of $\epsilon_{\rm mass}$ on stellar mass for both centrals and satellites, with more massive galaxies more efficiently mass quenched, regardless of the redshift. Another important information comes when comparing the two panels: while for central galaxies the dependence of $\epsilon_{\rm mass}$ on redshift is not clear, although it is stronger at higher redshift for very massive centrals ($\log M_* \gtrsim 11.3$), satellites in the intermediate/massive stellar mass range ($10 \lesssim \log M_* \lesssim 11$) are more efficiently quenched at lower redshift, while the trend reverts to that of high-mass centrals in the high-mass range.[6] These results are qualitatively in agreement with several observations (e.g., Darvish et al. 2016; Kawinwanichakij et al. 2017).

In order to quantify the accuracy of our model in predicting the observed relation between $\epsilon_{\rm mass}$ and stellar mass at different redshifts, in Figure 6 we show the predictions of our model (solid black lines) compared with the observed data by Kawinwanichakij et al. (2017; red crosses) in the redshift ranges $0.5 < z < 1.0$ (left panel) and $1.0 < z < 1.5$ (right panel). In the lowest redshift range, our model matches perfectly the observed data, while in the highest redshift range, although qualitatively it captures the observed trend, it fails quantitatively.

We now want to quantify the role of the environment on the mass quenching efficiency by plotting $\epsilon_{\rm mass}$ as a function of halo mass. This is shown in Figure 7, at different redshifts (different colors), and for galaxies in two stellar mass ranges (different panels), as shown in the legend. Analogously to Figure 3 for $\epsilon_{\rm env}$, we find that the mass quenching efficiency does not strongly depend on halo mass and only weakly on

[6] It must be noted that the predictions at very high stellar mass and at high redshift have to be taken with caution due to the poor statistics, especially for satellite galaxies.

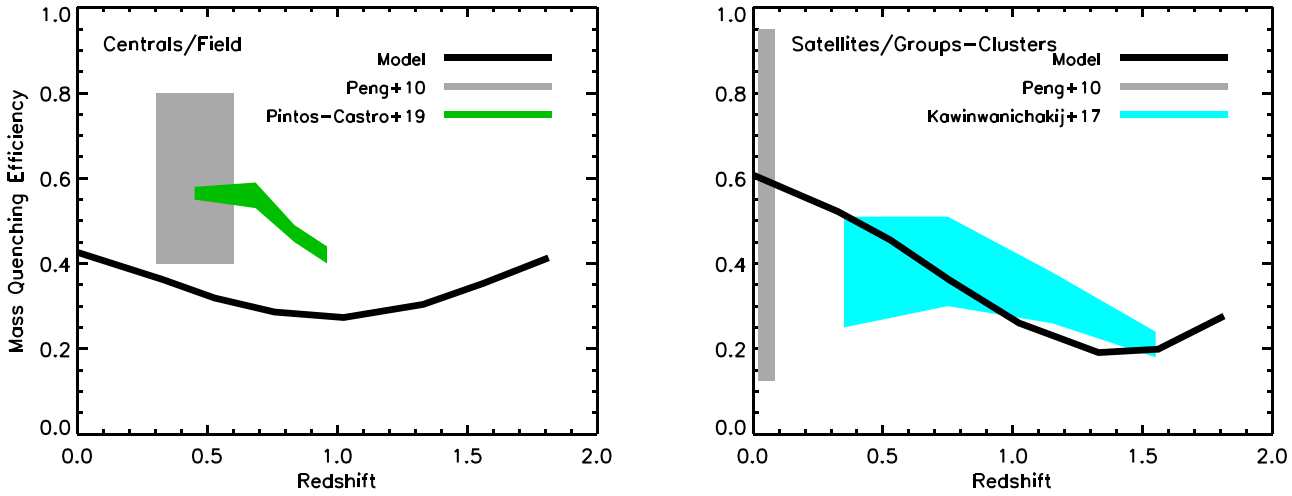

Figure 8. Mass quenching efficiency as predicted by the model (solid lines) as a function of redshift for central/field (left panel) and satellite/group-cluster galaxies (right panel), compared with several observed data. The results reflect those found in Figure 5 for both centrals (no clear trend with redshift) and satellites (decreasing efficiency with decreasing redshift). The model slightly underpredicts the mass quenching efficiency for central/field galaxies, while it captures the trend and matches the observed data for satellite/group-cluster galaxies.

redshift for the lowest stellar mass range, while it clearly depends on both in the highest stellar mass range. Then, this means that the environment (meant as the halo mass) has a strong influence on the mass quenching, another evidence that the two quenching modes are not separable. Moreover, by comparing Figures 3 and 7, we can note by eye that, for massive galaxies and regardless of the redshift, $\epsilon_{\rm mass}$ is always larger than $\epsilon_{\rm env}$, in good agreement with the observational results by Darvish et al. (2016).

To complete our analysis of $\epsilon_{\rm mass}$, we show in Figure 8 the integrated mass quenching efficiency, i.e., the total $\epsilon_{\rm mass}$ for galaxies with log $M* > 10.2$ (in order to have a fair comparison with the observed data shown), as a function of redshift, for central/field (left panel) and satellite/group-cluster (right panel) galaxies. The predictions of our model (solid lines) are compared with the observed data in the literature. The integrated mass quenching efficiency does not depend much on redshift in the case of central/field galaxies (which reflects the result found in Figure 5 for centrals), and our model underestimates the observed data available (Peng et al. 2010; Pintos-Castro et al. 2019). The stellar mass ranges on which the mass efficiency is calculated are comparable but not exactly the same,[7] which might be, at least in part, one possible reason for the mismatch. Other two possible reasons can be the different definitions of field/central galaxies and the separation between star-forming and quiescent galaxies. On the other hand, the model is able to catch the observed trend for satellite/group-cluster galaxies and to match the available observed data. Moreover, while centrals are mass quenched with roughly the same efficiency, around 0.4, satellites experience different mass quenching efficiencies with time, from around 0.2 at $z \sim 1.5$ to 0.6 at the present time, which means that $\epsilon_{\rm mass}$ is a factor of 3 times higher at $z = 0$ than it is at high redshifts. We will come back to this point in Section 4.2.

To summarize the most important results of this subsection, we can state that the mass quenching efficiency is dependent on redshift, stellar mass, and environmental dependent.

[7] For instance, the stellar mass range considered by Pintos-Castro et al. (2019) is $10.2 < \log M_* < 10.8$, while ours is log $M_* > 10.5$ because all centrals below that stellar mass are star-forming in our model.

4. Discussion

The aim of this work is to extend the results found in PapI by looking at the two quenching modes, due to internal processes that are linked to the stellar mass of a galaxy (mass quenching), and due to physical processes that are related to the surroundings of a galaxy (environmental quenching). These two processes together are believed to be responsible for the star formation history of galaxies and generally to act on different timescales. Quantifying their roles then becomes necessary if we want to understand which process/es are important and at what time for a galaxy with a given stellar mass. In the literature, there is no general consensus regarding what mode dominates and at which time, mainly because different authors look at different galaxy properties, which give opposing results.

In PapI, we studied the roles of mass and environment in quenching galaxies by analyzing the SFR and SSFR as a function of stellar mass, halo mass, and redshift. According to our analysis, the main conclusion was that mass quenching dominates at any redshift, while the environment plays only a marginal role. We stated that all the results could have been put together logically if environmental processes act very fast (Jung et al. 2018) in such a way that they do not affect the star formation activity, but can increase the probability of galaxies becoming quiescent. In the last decade, many authors have studied mass and environmental quenching by looking at their efficiencies (with all the caveats discussed above). The main pro of following such an approach comes from the fact that it is possible to quantify their effect, to provide numbers that can be compared. As mentioned above, the definitions of $\epsilon_{\rm mass}$ and $\epsilon_{\rm env}$ are quite arbitrary in the sense that any author can use their own proxy for the environment, which clearly makes comparisons not easy. However, despite that, any author can provide a range of numbers that can quantify the importance of the two modes and their dependence on time and on the main physical properties of galaxies such as stellar mass and their environment. Below, we discuss our analysis of $\epsilon_{\rm mass}$ and $\epsilon_{\rm env}$ with a full comparison with previous results and, more importantly, their implications. We focus on the dependence of $\epsilon_{\rm env}$ on redshift and environment, of $\epsilon_{\rm mass}$ on redshift and stellar mass,

and separately, their mutual dependence, i.e., $\epsilon_{\rm env}$ on stellar mass and $\epsilon_{\rm mass}$ on environment.

4.1. ϵ_{env} as a Function of Environment and Redshift

The environmental quenching efficiency has been studied by several authors (e.g., van den Bosch et al. 2008; Peng et al. 2010; Quadri et al. 2012; Balogh et al. 2016; Fossati et al. 2017 and many others), with results that at the time of the writing of this manuscript are still controversial (and the same applies for $\epsilon_{\rm mass}$). There is general agreement that $\epsilon_{\rm env}$ depends on the environment (meant either as clustercentric distance, local density, or halo mass), but not a full consensus on its dependence on redshift (see, e.g., Quadri et al. 2012; Balogh et al. 2016 for no dependence and, e.g., Fossati et al. 2017; Kawinwanichakij et al. 2017; Pintos-Castro et al. 2019 for dependence). However, there is more evidence that the environmental quenching efficiency depends on redshift. In Figure 4, we plot several observed data, which, put together, show the dependence of $\epsilon_{\rm env}$ on redshift. Despite that, even single studies find a clear trend with redshift. For example, Kawinwanichakij et al. (2017) explored the evolution of the environmental quenching efficiency with redshift for galaxies in different stellar mass bins, finding that it depends both on redshift and stellar mass. Similar conclusions have been reached by Pintos-Castro et al. (2019), who also show $\epsilon_{\rm env}$ versus redshift at different clustercentric distances and find that galaxies closer to the center have higher quenching efficiencies than those in the field.

Concerning the dependence on the environment, our model completely supports it. Because the environment is usually defined as either the local density (e.g., Kawinwanichakij et al. 2017) or as the clustercentric distance (e.g., Pintos-Castro et al. 2019), our analysis extends it to the halo mass. We show in Figure 3 that the halo mass acts in a different way in galaxies with different stellar mass. Low-mass galaxies ($\log M_* < 10.5$) suffer from environmental quenching independently of the fact that they reside in a $10^{13}\ M_\odot$ halo or a mature $10^{15}\ M_\odot$ cluster. On the other hand, high-mass galaxies are quenched differently depending on the halo mass of the object in which they reside, that is, clusters are more effective than groups or small groups in quenching high-mass galaxies. Finding the right physical mechanisms responsible for environmental quenching is beyond the scope of this paper. However, strangulation can be a possible candidate for low-mass galaxies, as it operates in all halos independently of their mass, while ram pressure stripping (but a contribution from strangulation can be an option) might be a good candidate for the quenching of massive galaxies, as it depends on the mass of the halo and it is stronger in more massive halos. Moreover, ram pressure stripping is stronger in the central regions of the clusters where, for dynamical reasons, more massive galaxies are supposed to fall into in a shorter time.

4.2. ϵ_{mass} as a Function of Stellar Mass and Redshift

The mass quenching efficiency $\epsilon_{\rm mass}$ has been found to be dependent on stellar mass and redshift by several authors (Darvish et al. 2016; Kawinwanichakij et al. 2017; Pintos-Castro et al. 2019), a result that agrees well with the prediction of our model. Most previous studies find $\epsilon_{\rm mass}$ to increase with cosmic time (as $\epsilon_{\rm env}$), in line with our predictions (see Figures 6–8) at least for satellites and in general for massive galaxies. The interesting point to highlight is the different evolution of $\epsilon_{\rm mass}$ with redshift for central and satellite galaxies. As pointed out in Section 3.2 and shown in Figure 8, centrals are quenched by internal processes with roughly the same efficiency, around 0.4, regardless of the redshift. This means that whatever processes are quenching these galaxies, they do not depend on the cosmic time. Processes such as supernova and AGN feedback can fit in the picture. On the other hand, satellites experience different mass quenching efficiencies with time, from around 0.2 at $z \sim 1.5$ to 0.6 at the present time, which means that $\epsilon_{\rm mass}$ is a factor of 3 times higher at $z = 0$ than it is at high redshifts. The obvious conclusion is that for galaxies in dense environments, the internal processes also suffer from environmental conditions and how they change with time, a hint that $\epsilon_{\rm mass}$ is dependent on environment. We will fully discuss this point below. The other important point for $\epsilon_{\rm mass}$ is its dependence on stellar mass. In agreement with previous work, our model also predicts that more massive galaxies are mass quenched more efficiently than less massive ones, independently of their rank, central or satellite, which is in line with the downsizing scenario where more massive galaxies quench faster (e.g., Popesso et al. 2011; Sobral et al. 2011; Fossati et al. 2017; Pintos-Castro et al. 2019; J. Rhee et al. 2020, in preparation).

4.3. The Mutual Dependence of ϵ_{env} and ϵ_{mass}

We now move the discussion to the main result of this work, that is, the mutual dependence of the two quenching efficiencies. Our analysis shows that the environmental quenching efficiency depends on stellar mass and, on the other hand, the mass quenching efficiency depends on the environment, meaning that the two quenching efficiencies are not separable. There is not yet agreement on this important point. Some authors find evidence that they are separable, such as Baldry et al. (2006), van den Bosch et al. (2008), Peng et al. (2010), Quadri et al. (2012), Kovač et al. (2014), and van der Burg et al. (2018), and that they are not, such as Balogh et al. (2016), Darvish et al. (2016), Fossati et al. (2017), Jian et al. (2017), Kawinwanichakij et al. (2017), Papovich et al. (2018), and Pintos-Castro et al. (2019). Given the importance of the point, it is worth discussing the results of a few of the above works. Most of the first studies that focused on the quenching efficiencies argue that the quenching given by the environmental processes is not influenced by the stellar mass of the galaxies and, vice versa, that the quenching given by internal processes that are linked to the stellar mass of galaxies is not dependent on the particular environment galaxies are living in. This has been shown by Peng et al. (2010) out to $z \sim 1$, followed by an extension to $z \sim 1.8$ by Quadri et al. (2012). Peng et al. (2010) use a sample of galaxies drawn from the Sloan Digital Sky Survey and zCOSMOS and find that the mass quenching efficiency is completely independent of environment meant as local density, and the environmental quenching efficiency is independent of stellar mass. Quadri et al. (2012), who used a mass-selected sample from the UKIDSS Ultra-Deep Survey, echo Peng et al.'s results for $\epsilon_{\rm env}$ and extend them to higher redshifts. More recently, van der Burg et al. (2018), who study a sample of 21 clusters at $z \sim 0.6$ (on average) detected by *Planck*, find that the environmental quenching efficiency is independent of stellar mass in any environment, although it increases toward the inner regions of the clusters.

However, over the last few years, there have been more evidence in support of the fact that the efficiencies of the two quenching modes are not separable. Balogh et al. (2016) analyze galaxies in groups and clusters at $0.8 < z < 1.2$ from the GCLASS and GEEC2 surveys and find that $\epsilon_{\rm env}$ (called conversion fraction in their paper) is nearly independent of stellar mass for galaxies more massive than $\log M_* \sim 10.3$, but it decreases at lower stellar mass, becoming consistent with zero at $\log M_* \sim 9.5$. The inefficiency of the environment in quenching low -mass galaxies has been pointed out also by Papovich et al. (2018). As introduced above, these authors study the evolution of the stellar mass functions of quiescent and star-forming galaxies in a wide redshift range and argue that a mass-invariant $\epsilon_{\rm env}$ in the low-mass end, below $\log M_* \sim 9.5$, should end up in a steeper slope of the stellar mass function of quiescent galaxies than observed. They then conclude that in the range $0.5 < z < 1.5$, the environmental quenching efficiency must decrease with stellar mass. With the same set of data, Kawinwanichakij et al. (2017) find the same result by looking directly at $\epsilon_{\rm env}$. Very recently, Pintos-Castro et al. (2019) confirmed all these results concerning the mutual dependence of the quenching modes. They take advantage of a sample of more than 200 clusters IR-selected from the ELAIS-N1 and *XMM*-LSS fields in the redshift range $0.3 < z < 1.1$. By using the clustercentric distance as a proxy of the environment, they find that both efficiencies depend on stellar mass and environment, in good agreement with the above-mentioned works and our analysis.

One question arises in very naturally: why is the mutual dependence of the two quenching modes still controversial? Our analysis clearly supports the picture where both efficiencies are dependent on environment and stellar mass, as did many of the works quoted above. We agree with the argument of Papovich et al. (2018), i.e., the reason can be found in the stellar mass limit probed by different observations. For instance, those studies that argue for a mass-invariant environmental quenching efficiency (e.g., Peng et al. 2010; Quadri et al. 2012; Kovač et al. 2014) are limited to moderate stellar mass, $\log M_* \gtrsim 10$ in most of the cases. To shed light on this point, we need more observations that can probe lower stellar masses, $\log M_* \sim 9$–9.5.

5. Conclusions

Taking advantage of an analytic model of galaxy formation that was set to match the evolution of the global stellar mass function from high redshift to the present time and to give, at the same time, good predictions of the evolution of the SFR–M_* relation, we have investigated the galaxy quenching efficiencies due to environment and stellar mass. These two quenching modes have been analyzed in detail, by looking at their dependence on redshift, stellar mass, and halo mass (which we have used as a proxy for the environment). Given the result outlined from our analysis, we conclude as follows:

1. The environmental quenching efficiency $\epsilon_{\rm env}$ is a function of halo mass, stellar mass, and redshift. The efficiency increases with cosmic time and generally with halo mass. These trends are very neat for galaxies more massive than $\log M_* \sim 10.5$, while for less massive galaxies, we do find an increase with redshift, but a constant relation with halo mass at fixed redshift. $\epsilon_{\rm env}$ depends on stellar mass. At low stellar mass, below $\log M_* \sim 9.5$, the efficiency is consistent with zero. It rapidly increases and reaches the highest values at $\log M_* \sim 10.5$ (depending on the redshift), to drop again at higher stellar mass.
2. The mass quenching efficiency is also a function of stellar mass, halo mass, and redshift. For central galaxies, it strongly depends on stellar mass, being much higher for more massive centrals, but very weakly on redshift. Similarly, for satellite galaxies, $\epsilon_{\rm mass}$ is in a strong relationship with stellar mass, and also with redshift in the intermediate stellar mass range ($10 \lesssim \log M_* \lesssim 11$) since $z < 1.5$. Moreover, the mass quenching efficiency of galaxies more massive than $\log M_* \sim 10.5$ depends on environment at any redshift, being higher in more massive halos, while it is constant (with different values depending on the redshift) for less massive galaxies.
3. In previous works that studied the two quenching efficiencies, the environment is usually defined as either the local density or as the clustercentric distance. Our analysis extends it to the halo mass, showing that this is also a good proxy for the environment.
4. The stellar mass and environmental quenching efficiencies are not separable, at any redshift investigated. $\epsilon_{\rm env}$ depends on stellar mass, and vice versa, $\epsilon_{\rm mass}$ (for massive galaxies) depends on the environment. This means that, according to our analysis, intermediate-mass galaxies are environmentally quenched faster, and, on the other hand, intermediate/massive galaxies in more massive halos quench faster.
5. Mass quenching mechanisms dominate the quenching of massive galaxies at any redshift, while the environment becomes gradually more important as time goes by in the intermediate stellar mass range and dominates at lower stellar masses, $\log M_* < 10$. At stellar masses lower than $\log M_* \lesssim 9.5$, both quenching mechanisms become inefficient, regardless of the redshift.

The predictions of our model agree qualitatively well with the results of most of the studies quoted above. The general picture supported and proved by this analysis sees the two quenching modes to be dependent on stellar mass, environment, and redshift. In the context of "nature" versus "nurture," these results prove that they are both important for galaxy evolution, interconnected in a nontrivial way. The redshift, stellar mass, and halo mass dependences of both quenching modes for galaxies in groups and clusters are particularly interesting because they highlight the need to invoke a plethora of physical processes that act with different timescales, at different stellar masses and halo mass scales. Starvation and ram pressure stripping are good candidates for the environment-driven processes, while, except for AGN and supernova feedback, most of the difference in the quenching due to internal processes can arise from the fraction pf stellar/gas mass that galaxies have at the time of accretion.

The authors thank the anonymous referee for constructive comments which helped to improve the manuscript. This work is supported by the National Key Research and Development Program of China (No. 2017YFA0402703), by the National Natural Science Foundation of China (Key Project No. 11733002), and the NSFC grant (11825303, 11861131006). S.K.Y. acknowledges support from the Korean National Research Foundation (NRF-2017R1A2A05001116).

ORCID iDs

E. Contini https://orcid.org/0000-0002-2873-8598
Q. Gu https://orcid.org/0000-0002-3890-3729
X. Ge https://orcid.org/0000-0002-8348-2783
J. Rhee https://orcid.org/0000-0002-0184-9589
S. K. Yi https://orcid.org/0000-0002-4556-2619

References

Baldry, I. K., Balogh, M. L., Bower, R. G., et al. 2006, MNRAS, 373, 469
Baldry, I. K., Glazebrook, K., Brinkmann, J., et al. 2004, ApJ, 600, 681
Balogh, M., Eke, V., Miller, C., et al. 2004, MNRAS, 348, 1355
Balogh, M. L., McGee, S. L., Mok, A., et al. 2016, MNRAS, 456, 4364
Bamford, S. P., Nichol, R. C., Baldry, I. K., et al. 2009, MNRAS, 393, 1324
Blanton, M. R., Hogg, D. W., Bahcall, N. A., et al. 2003, ApJ, 594, 186
Bremer, M. N., Phillipps, S., Kelvin, L. S., et al. 2018, MNRAS, 476, 12
Brinchmann, J., Charlot, S., White, S. D. M., et al. 2004, MNRAS, 351, 1151
Cassata, P., Cimatti, A., Kurk, J., et al. 2008, A&A, 483, L39
Chabrier, G. 2003, PASP, 115, 763
Chartab, N., Mobasher, B., Darvish, B., et al. 2019, arXiv:1912.04890
Cicone, C., Maiolino, R., Sturm, E., et al. 2014, A&A, 562, A21
Contini, E., De Lucia, G., Villalobos, Á., & Borgani, S. 2014, MNRAS, 437, 3787
Contini, E., Gu, Q., Kang, X., et al. 2019a, ApJ, 882, 167
Contini, E., Kang, X., Romeo, A. D., & Xia, Q. 2017a, ApJ, 837, 27
Contini, E., Kang, X., Romeo, A. D., Xia, Q., & Yi, S. K. 2017b, ApJ, 849, 156
Contini, E., Yi, S. K., & Kang, X. 2018, MNRAS, 479, 932
Contini, E., Yi, S. K., & Kang, X. 2019b, ApJ, 871, 24
Cooke, E. A., Hatch, N. A., Stern, D., et al. 2016, ApJ, 816, 83
Cooper, M. C., Gallazzi, A., Newman, J. A., & Yan, R. 2010, MNRAS, 402, 1942
Croton, D. J., Springel, V., White, S. D. M., et al. 2006, MNRAS, 365, 11
Dalla Vecchia, C., & Schaye, J. 2008, MNRAS, 387, 1431
Darvish, B., Mobasher, B., Sobral, D., et al. 2016, ApJ, 825, 113
Davies, L. J. M., Robotham, A. S. G., Lagos, C. d. P., et al. 2019, MNRAS, 483, 5444
Dekel, A., & Silk, J. 1986, ApJ, 303, 39
Dressler, A. 1980, ApJ, 236, 351
Fabian, A. C. 2012, ARA&A, 50, 455
Fang, J. J., Faber, S. M., Koo, D. C., & Dekel, A. 2013, ApJ, 776, 63
Fossati, M., Wilman, D. J., Mendel, J. T., et al. 2017, ApJ, 835, 153
Gallazzi, A., Brinchmann, J., Charlot, S., & White, S. D. M. 2008, MNRAS, 383, 1439
Gunn, J. E., & Gott, J. R., III 1972, ApJ, 176, 1
Jian, H.-Y., Lin, L., Lin, K.-Y., et al. 2017, ApJ, 845, 74
Jung, S. L., Choi, H., Wong, O. I., et al. 2018, ApJ, 865, 156
Kang, X., Li, M., Lin, W. P., & Elahi, P. J. 2012, MNRAS, 422, 804
Kauffmann, G., Heckman, T. M., White, S. D. M., et al. 2003, MNRAS, 341, 33
Kauffmann, G., White, S. D. M., Heckman, T. M., et al. 2004, MNRAS, 353, 713
Kawinwanichakij, L., Papovich, C., Quadri, R. F., et al. 2017, ApJ, 847, 134
Kawinwanichakij, L., Quadri, R. F., Papovich, C., et al. 2016, ApJ, 817, 9
Knobel, C., Lilly, S. J., Kovač, K., et al. 2013, ApJ, 769, 24
Kovač, K., Lilly, S. J., Knobel, C., et al. 2014, MNRAS, 438, 717
Laganá, T. F., & Ulmer, M. P. 2018, MNRAS, 475, 523
Larson, R. B. 1974, MNRAS, 169, 229
Larson, R. B., Tinsley, B. M., & Caldwell, C. N. 1980, ApJ, 237, 692
Moore, B., Katz, N., Lake, G., Dressler, A., & Oemler, A. 1996, Natur, 379, 613
Muzzin, A., Marchesini, D., Stefanon, M., et al. 2013, ApJ, 777, 18
Muzzin, A., Wilson, G., Yee, H. K. C., et al. 2012, ApJ, 746, 188
Nantais, J. B., van der Burg, R. F. J., Lidman, C., et al. 2016, A&A, 592, A161
Noeske, K. G., Weiner, B. J., Faber, S. M., et al. 2007, ApJL, 660, L43
Omand, C. M. B., Balogh, M. L., & Poggianti, B. M. 2014, MNRAS, 440, 843
Pallero, D., Gómez, F. A., Padilla, N. D., et al. 2019, MNRAS, 488, 847
Papovich, C., Kawinwanichakij, L., Quadri, R. F., et al. 2018, ApJ, 854, 30
Peng, Y.-j., Lilly, S. J., Kovač, K., et al. 2010, ApJ, 721, 193
Peng, Y.-j., Lilly, S. J., Renzini, A., & Carollo, M. 2012, ApJ, 757, 4
Pintos-Castro, I., Yee, H. K. C., Muzzin, A., Old, L., & Wilson, G. 2019, ApJ, 876, 40
Popesso, P., Rodighiero, G., Saintonge, A., et al. 2011, A&A, 532, A145
Quadri, R. F., Williams, R. J., Franx, M., et al. 2012, ApJ, 744, 88
Sobral, D., Best, P. N., Smail, I., et al. 2011, MNRAS, 411, 675
Vale, A., & Ostriker, J. P. 2004, MNRAS, 353, 189
van den Bosch, F. C., Aquino, D., Yang, X., et al. 2008, MNRAS, 387, 79
van der Burg, R. F. J., McGee, S., Aussel, H., et al. 2018, A&A, 618, A140
van der Burg, R. F. J., Muzzin, A., Hoekstra, H., et al. 2013, A&A, 557, A15
van der Wel, A., Franx, M., van Dokkum, P. G., et al. 2014, ApJ, 788, 28
von der Linden, A., Wild, V., Kauffmann, G., White, S. D. M., & Weinmann, S. 2010, MNRAS, 404, 1231
Weinmann, S. M., van den Bosch, F. C., Yang, X., & Mo, H. J. 2006, MNRAS, 366, 2
Wetzel, A. R., Tinker, J. L., & Conroy, C. 2012, MNRAS, 424, 232
Wetzel, A. R., Tinker, J. L., Conroy, C., & van den Bosch, F. C. 2013, MNRAS, 432, 336
Wuyts, S., Förster Schreiber, N. M., van der Wel, A., et al. 2011, ApJ, 742, 96